



UNIVERSITÀ
DEGLI STUDI
FIRENZE

FLORE

Repository istituzionale dell'Università degli Studi di Firenze

Enhancement of the Magnetic Coupling in Exfoliated CrCl₃ Crystals Observed by Low-Temperature Magnetic Force Microscopy and X-ray

Questa è la Versione finale referata (Post print/Accepted manuscript) della seguente pubblicazione:

Original Citation:

Enhancement of the Magnetic Coupling in Exfoliated CrCl₃ Crystals Observed by Low-Temperature Magnetic Force Microscopy and X-ray Magnetic Circular Dichroism / Serri M.; Cucinotta G.; Poggini L.; Serrano G.; Saintavit P.; Strychalska-Nowak J.; Politano A.; Bonaccorso F.; Caneschi A.; Cava R.J.; Sessoli R.; Ottaviano L.; Klimczuk T.; Pellegrini V.; Mannini M.. - In: ADVANCED MATERIALS. - ISSN 0935-9648. -

Availability:

The webpage <https://hdl.handle.net/2158/1218986> of the repository was last updated on 2022-02-17T18:39:43Z

Published version:

DOI: 10.1002/adma.202000566

Terms of use:

Open Access

La pubblicazione è resa disponibile sotto le norme e i termini della licenza di deposito, secondo quanto stabilito dalla Policy per l'accesso aperto dell'Università degli Studi di Firenze (<https://www.sba.unifi.it/upload/policy-oa-2016-1.pdf>)

Publisher copyright claim:

Conformità alle politiche dell'editore / Compliance to publisher's policies

Questa versione della pubblicazione è conforme a quanto richiesto dalle politiche dell'editore in materia di copyright.

This version of the publication conforms to the publisher's copyright policies.

La data sopra indicata si riferisce all'ultimo aggiornamento della scheda del Repository FloRe - The above-mentioned date refers to the last update of the record in the Institutional Repository FloRe

(Article begins on next page)

Title Enhancement of the Magnetic Coupling in Exfoliated CrCl₃ Crystals Observed by Low Temperature Magnetic Force Microscopy and X-Ray Circular Dichroism.

Michele Serri^{1}, Giuseppe Cucinotta², Lorenzo Poggini², Giulia Serrano^{2,3}, Philippe Sainctavit^{4,5}, Judyta Strychalska-Nowak⁶, Antonio Politano^{7,8}, Francesco Bonaccorso^{1,9}, Andrea Caneschi³, Robert J. Cava¹⁰, Roberta Sessoli², Luca Ottaviano^{7,8}, Tomasz Klimczuk⁶, Vittorio Pellegrini^{1,9}, Matteo Mannini^{2*}*

Dr. M. Serri, Dr. F. Bonaccorso, Dr. V. Pellegrini
Istituto Italiano di Tecnologia – Graphene Labs, via Morego 30, 16163 Genova, Italy
E-mail: michele.serri@iit.it

Dr. L. Poggini, Dr. G. Cucinotta, Dr. G. Serrano, Prof. R. Sessoli, Prof. M. Mannini
Università degli studi di Firenze, Chemistry Department “U.Schiff” & INSTM RU, Via della
Lastruccia 3-13, 50019 Sesto Fiorentino, Italy
E-mail: matteo.mannini@unifi.it

Dr. G. Serrano, Prof. A. Caneschi
Università degli Studi di Firenze, Department of Industrial Engineering, DIEF, & INSTM RU,
Via di S. Marta 3, 50139 Firenze, Italy

Dr. Ph. Sainctavit
Institut de Mineralogie, de Physique des Matériaux et de Cosmochimie, UMR 7590, CNRS,
Sorbonne Université, MNHN, F-75005 Paris, France.
Synchrotron SOLEIL, L’Orme des Merisiers, Saint-Aubin—BP 48, F-91192 Gif-sur-Yvette,
France

J. Strychalska-Nowak, Prof. Tomasz Klimczuk
Gdansk University of Technology, Faculty of Applied Physics and Mathematics, 80-233
Gdansk, Poland

Dr. A. Politano, Prof. L. Ottaviano
Università dell’Aquila, Dipartimento di Scienze Fisiche e Chimiche (DSFC), Via Vetoio 10,
67100 L’Aquila, Italy

Prof. L. Ottaviano
CNR-SPIN UoS L’Aquila, Via Vetoio 46, 67100 L’Aquila, Italy

Dr. F. Bonaccorso, Dr. V. Pellegrini
BeDimensional Spa, 16163 Genoa, Italy

Prof. Robert J. Cava
Department of Chemistry Princeton University, Princeton, NJ 08544, USA

Keywords: magnetism, van der Waals, honeycomb-lattice, MFM, spintronics

ABSTRACT

Magnetic crystals formed by 2D layers interacting by weak van der Waals forces are currently a hot research topic. When these crystals are thinned to nanometric size, they can manifest strikingly different magnetic behavior compared to the bulk form. This can be the result of, for example, quantum electronic confinement effects, or the presence of defects or pinning of the crystallographic structure in metastable phases induced by the exfoliation process. In this work, we perform an investigation of the magnetism of micromechanically cleaved CrCl_3 flakes with thickness >10 nm. These flakes were characterized by superconducting quantum interference device magnetometry, surface-sensitive X-ray magnetic circular dichroism and spatially resolved magnetic force microscopy. Our results highlight an enhancement of the CrCl_3 antiferromagnetic interlayer interaction that appears to be independent from the flake size when the thickness is tens of nm. The estimated exchange field is 9 kOe, representing an increase of $\sim 900\%$ compared to the one of the bulk crystal. This effect can be attributed to the pinning of the high-temperature monoclinic structure, as recently suggested by polarized Raman spectroscopy investigations in thin (8-35 nm) CrCl_3 flakes.

MAIN TEXT

Layered crystals held together by van der Waals (vdW) forces feature peculiar physical properties due to the unbalance between the strong in-plane interactions, determined by the two-dimensional network of covalent bonds, and the weak interlayer ones. Top-down exfoliation and bottom-up growth protocols used in such materials permit to produce high aspect ratio 2D crystals with thicknesses down to single or few atomic layers.^[1] A large number of vdW materials has been studied experimentally or theoretically, finding an abundance of different functional properties that can also be tuned depending on the thickness of the produced samples.^[2,3] Recently, vdW materials that exhibit ferromagnetic order in ultrathin crystals^[4-7] have attracted increasing attention as potential building blocks of

spintronic devices in 2D heterostructures.^[8–12] In these devices, the spin degree of freedom is controlled and manipulated in order to enable new quantum modes of operation for logic devices^[11,13] and sensors^[14,15] improving efficiency and speed.^[16] Among magnetic materials interesting for 2D scalability,^[17] chromium trihalides (CrX_3) crystals represent a class of semiconducting layered materials with potential applications in opto-electronics^[12] and spintronics,^[11,13–15,18,19] e.g., as circularly polarized light emitters^[12] and magnetic tunnel junctions.^[19–21] Individual layers of CrX_3 are composed by a Cr sheet forming a honeycomb net, sandwiched between two halide sheets, where Cr^{3+} cations in $S = 3/2$ spin state are octahedrally coordinated by 6 halide X^- anions, and each anion is shared between two cations (**Figure 1a,b**) resulting in an intra-layer ferromagnetic exchange interaction.^[22] Two types of layer stacking arrangement, monoclinic and rhombohedral, have been observed in bulk CrX_3 crystals, depending on the X element and temperature.^[23] The investigation of the effect of nanostructuring (i.e., in both lateral size and thickness) and exfoliation processes on the magnetic properties of these vdW materials is crucially important for their exploitation in spintronic devices.

Several reports^[4,13–15] have shown that thin (0.7–14 nm, i.e., 1–20 layers) CrI_3 flakes exhibit antiferromagnetic interlayer coupling, in contrast with the ferromagnetic interaction in the bulk counterpart.^[24] As of late, a ten-fold enhancement of antiferromagnetic exchange was reported in exfoliated CrCl_3 few layer (1–4) flakes compared to the pristine bulk crystal.^[21] Experimental evidence suggests that interlayer magnetism is insensitive to the thickness of the CrX_3 exfoliated flakes, at least when this is less than ≈ 14 nm.^[14] Recent experimental^[21] and theoretical^[10,25,26] investigations have suggested that the magnetic properties of the exfoliated CrX_3 flakes derive from a crystallographic difference from the pristine bulk crystals.^[10,21,25,26] In fact, *ab initio* calculations predict a stronger antiferromagnetic exchange in the monoclinic phase compared to the rhombohedral one,^[10,25,26] while polarized Raman experiments (at the $\approx 247 \text{ cm}^{-1}$ mode) on CrCl_3 flakes (8–35 nm)^[21] indicate the absence of the low temperature

($T < 235$ K) rhombohedral phase, which is contrarily observed in bulk.^[27] The origin of this phenomenon is still under debate. It has been speculated that the phase transition is hindered in the exfoliated flakes by stacking faults and other defects induced by the exfoliation process.^[21] An alternative explanation invokes the existence of a surface phase on CrX_3 crystals, which is found both in exfoliated and pristine crystals, but is masked in the latter by the prevailing bulk phase.^[14] A deeper investigation of these materials, based on the comparison of bulk magnetometric analysis with the information achieved through surface-sensitive magnetic techniques, is mandatory for a sound assignment of the local magnetic state.

Here, we unravel the magnetic properties of micromechanically cleaved chromium trichloride (CrCl_3) crystals having thickness of the order of tens of nm. We use low temperature magnetic force microscopy (MFM), as a local magnetic probe, flanked by angle-resolved X-ray magnetic circular dichroism (XMCD) and superconducting quantum interference device (SQUID) magnetometry. While previous studies focused on the magnetism of ultrathin flakes (< 9 nm),^[21,28,29] our multi-technique study presents a detailed characterization of pristine and exfoliated CrCl_3 in the thickness range ≈ 10 – 50 nm. Our results show that micromechanical cleavage determines, even at the mesoscopic thickness of 10–50 nm thickness - a scale of technological relevance - a significant change in the magnetic properties of the CrCl_3 crystal. A clear example is the increase of the saturation field at low-temperature (4 K – 14 K) compared to the bulk counterpart. Besides, these changes are not associated with an anomalous behavior of the surface layers.

Chromium trichloride (CrCl_3) is the most stable among the chromium trihalide materials, offering significant advantages in processability compared to the iodide and bromide ones, which suffer from rapid (< 15 min for CrI_3) attack by atmospheric air.^[14] In the bulk form, CrCl_3 layers at room temperature are stacked according to a monoclinic phase (space group $C2/m$, **Figure 1a** and **Figure 1b**), as confirmed here by the X-ray diffraction

pattern (see **Figure S1**) and the detected Raman modes (**Figure S2**). Bulk CrCl_3 crystals exhibit at low temperature ($\sim 15\text{K}$) two magnetic transitions that we observed by temperature dependent dc magnetic susceptibility (χ_{dc}) measurements (**Figure 1d**). The maximum of the slope ($-\text{d}\chi/\text{dT}$) at 15.2 K and 15.5 K, detected with the field in-plane, *i.e.* parallel to CrCl_3 layers and the crystal *ab* plane (Figure 1d), and out-of-plane (**Figure S3a**) respectively, identifies the paramagnetic-2D ferromagnetic transition temperature $T_{\text{C}}^{[30]}$ which results in ferromagnetic order within individual layers. The transition from 2D ferromagnetic to 3D antiferromagnetic, *i. e.* the antiparallel arrangement of the moments of neighboring layers, is picked up by the zero of $\text{d}\chi_{\text{dc}}/\text{dT}$ at $T_{\text{N}}=13\text{ K}$ (field in-plane) and 13.7 K (field out-of-plane). These magnetic transitions can also be revealed by ac susceptibility measurements^[31] (Figure 1d, Figure S3 a). The transitions are sensitive to the internal field; therefore different values of the external field (here 1 kOe) or crystal orientations (due to demagnetizing factors) yield slightly different transition temperatures, which can justify the slight differences with literature values ($T_{\text{C}} \approx 17\text{ K}$, $T_{\text{N}} = 15.5\text{ K}$).^[27,32–34] As expected, isothermal magnetization curves of the bulk crystal (**Figure 1e**, **Figure S3b**) are in agreement with previous studies.^[27,32,33] At 4 K the in-plane magnetization rises linearly with field, corresponding to the progressive canting of the magnetization of the two antiferromagnetically coupled sublattices, until, at field strength $H_{\text{FM}} \approx 2\text{ kOe}$, the magnetic sublattices become aligned with the external field in a ferromagnetic-like state. Above H_{FM} , the magnetization increases until reaching a saturation moment of 3 Bohr magnetons (μ_{B}) per Cr atom (μ_{B}) at 30 kOe, in agreement with $S = 3/2$ for a trivalent Cr.

To investigate flakes, a CrCl_3 bulk crystal was exfoliated inside a nitrogen-filled glovebox, by repeated cleaving with an adhesive PDMS film (**Figure 1 c**). The exfoliated CrCl_3 flakes were transferred onto a Si (100) chip and onto a Kapton adhesive tape. The CrCl_3 flakes on Si were analysed by atomic force and optical microscopy, determining a thickness

of 35 ± 20 nm with lateral sizes of 4 ± 2 μm (see **Figure S4**). The chemical stability of the exfoliated crystals deposited onto Si was confirmed by X-ray photoelectron spectroscopy (XPS) in the Cr 2p and Cl 2p regions, which shows virtually identical components in bulk and exfoliated CrCl_3 flakes, and in line with what reported for polycrystalline samples (see X-ray photoelectron spectroscopy section, **Figure S5** and **Table S1**).^[35]

The magnetic properties of flakes on Kapton were first evaluated using SQUID magnetometry limited to the in-plane field configuration (see Figure 1d and Methods for details). The temperature dependence of χ_{dc} (Figure 1d) evidences the persistence of the magnetic transitions noticed in the pristine CrCl_3 material. In particular, the ferromagnetic transition (determined from $d\chi/dT$) is observed in these flakes at 16 K, while antiferromagnetic one at 13.6 K. Notably, differences of the exfoliated CrCl_3 flakes compared to the bulk sample can be found in the isothermal magnetization curves (Figure 1e), revealing that thinning by exfoliation affects the in-plane magnetic properties of the crystal. The magnetization in the exfoliated CrCl_3 flakes rises with the applied field at a slower rate compared to the bulk. The curve changes slope at 2 kOe, indicating the presence of multiple contributions. These could be explained by the presence of CrCl_3 flakes with different thicknesses, a part of them still exhibiting a bulk-like behaviour.

To gain insights into the magnetic behaviour of the CrCl_3 flakes, we performed low temperature XMCD investigations (**Figure 2a** and **S6**). X-ray magnetic circular dichroism overcomes the limits of traditional magnetometry in terms of both selectivity and sensitivity because the dichroic signal for transition metal-based systems is, in a good approximation, proportional to the average magnetic moment of the absorbing element at the temperature, field strength and relative orientation of the sample with respect to the X-ray beam direction of the investigation.^[36] X-ray absorption spectroscopy (XAS) spectra were recorded with opposite circularly polarized light at 4 K and 14 K under an external magnetic field of 30 kOe at the Cr $L_{2,3}$ edges.^[37,38] We observe a strong negative dichroic signal at 575.9 eV that, for

normal incidence, corresponds to $\sim 120\%$ (**Figure S7**) and $\sim 128\%$ (Figure 2a) of the edge-jump for the bulk crystal and the exfoliated flakes, respectively, consistent with a magnetic moment of about $3 \mu_B$ per Cr atom.^[39,40] X-ray absorption spectroscopy and XMCD line shapes are in agreement with an octahedral Cr^{3+} found in other compounds (**Figure S8**).^[41,42]

The value of the maximum of the XMCD signal was then monitored during a sweep of the magnetic field between 30 kOe and -30 kOe to obtain the magnetization curve ($I_{\text{XMCD}}(H)$) of the CrCl_3 flakes (**Figure 2b** and **Figure 2c**). These measurements were performed at normal (0°) and grazing (60°) incidence, with respect to the sample surface, to highlight the differences between the out-of-plane and in-plane behaviour of the flakes. These differences were not accessible through SQUID measurements due to experimental constraints. At grazing incidence (whose configuration mostly resembles the SQUID in-plane measurements) the $I_{\text{XMCD}}(H)$ (Figure 2b) is qualitatively similar to the $M(H)$ measured on the CrCl_3 flakes on Kapton at 4 K and 14 K (Figure 1e). In particular, one can recognize a similar change of the slope around 2 kOe, followed by an almost linear increase in the magnetization, which approaches saturation just below 20 kOe. The $I_{\text{XMCD}}(H)$ curve obtained at normal incidence (Figure 2c) shows an analogous behaviour, which overlaps almost perfectly with the measurement at grazing incidence after accounting for the anisotropy due to the flakes aspect ratio (**Figure S9**, see Demagnetizing field correction methods). The agreement between the SQUID and variable magnetic field XMCD characterizations on the exfoliated samples is striking. It confirms that the micromechanical cleavage of the crystal to obtain CrCl_3 flakes with nanometric thickness induces a modification of the low-temperature magnetic properties of the material, rather than increasing surface effects.

Magnetic force microscopy maps gradients of the stray field of the magnetized sample.
^[43] The MFM signal at each point is proportional to the local magnetization of the flake times a geometric factor that depends on the magnetization of the tip and its relative position with respect to the flake. Previous works by our group and others have shown that this technique

can be used to obtain magnetization curves of magnetic microstructures of molecular magnets, provided that either the tip magnetization does not change during the field scan or its change is well characterized.^[44,45]

Here, in order to characterize the magnetic behaviour of individual flakes and locally discriminate the contribution of flake thickness, we performed in parallel AFM and MFM measurements (Figure 3). We adopted the same preparation procedure of the flakes on silicon described above and we performed MFM characterization at 14 K, close to the χ maximum. **Figure 3a** shows the AFM image of the sample. The feature at the centre of the area may consist of two overlapping CrCl_3 flakes or a single folded flake of ≈ 25 nm thickness. A perpendicular (out-of-plane) magnetic field of 50 kOe at 14 K was applied and a map of the magnetic force was acquired at a probe lift height of 100 nm. A clear magnetic contrast is observed in **Figure 3b**, highlighting regions of attractive magnetic interaction inside the flakes and repulsive force just outside the border of the flakes. The findings are consistent with the fact that the CrCl_3 flakes are perpendicularly magnetized by the field, which creates a re-entrant stray field outside of the flakes. As expected, the MFM signal reaches its maximum in regions where the magnetization or the thickness is discontinuous, such as the flake borders, while it is minimum inside the flakes, akin to a uniformly magnetized infinite plane, which does not generate any stray field.^[46] Magnetic force microscopy measurements repeated at decreasing field strengths have shown progressive fading of the magnetic features (**Figure 3c**). A very weak contrast is still observable after a demagnetization cycle, which must be attributed to spurious electrostatic or van der Waals forces, despite compensation of the contact potential (for more details see magnetic force microscopy methods in supplementary material). To quantitatively monitor the magnetic contrast as a function of the field we have followed a similar protocol adopted for a patterned deposit of single molecule magnets.^[44] We estimated the MFM contrast from spatial profiles of the frequency shift maps along three paths, indicated by the dotted lines in the topography and MFM images (see Figure 3a and

Figure 3b). As noticed from the topographic contrast, the selected paths intersect regions of different height (**Figure 3d**, bottom), thus justifying the complex dependence on the spatial coordinate of the corresponding MFM profiles shown at the top of Figure 3d. However, one can extract from this data a contrast Δf defined here as the difference between the maximum and the minimum of the MFM signal detected around the lower edge of the flake. By studying the field dependence of Δf we observe similar trends in all of the three profiles considered, as highlighted in **Figure 3e** by the overlap of the MFM contrast curves after normalization. This behaviour is in line with the one observed with the average measurements on the exfoliated material; for instance the $\Delta f(H)$ curve extracted from one of these sets (path 1, thickness = 32 ± 3 nm) almost perfectly overlaps with the 14 K XMCD data at normal incidence (Figure 2c). Our results suggest that the saturation field of the CrCl_3 flakes is independent of the number of layers in the range of thickness considered here. We also found that the saturation value of Δf , that is proportional to the aerial density of magnetic moment of the flake at saturation, follows, as expected, an apparent linear dependence with respect to the flake thickness (see **Figure 3f**). An offset of ~ 5 nm to the “true” thickness value can be explained by the additional height introduced by the interface between the flake and the substrate.^[47]

Our study highlights MFM as a key technique for the investigation of 2D materials. While SQUID magnetometry probed the whole ensemble of exfoliated flakes, MFM provided magnetic and topographic information with nanometric resolution that were used to correlate the behaviour of flakes with their thickness. Compared to magneto-optical methods, MFM has higher spatial resolution and offers a simultaneous measurement of the flake area and thickness, facilitating systematic investigations of size-dependent effects in 2D magnets.

The results of the MFM characterization support our interpretation of the XMCD and SQUID results, and the hypothesis that the exfoliated CrCl_3 flakes with a thickness of tens of nm exhibit magnetic saturation at higher fields compared to the bulk counterpart. This difference could be due to magnetic interactions contrasting the alignment of the spins with the magnetic

field, such as an increase of the antiferromagnetic exchange term or of the magneto-crystalline anisotropy compared to the unexfoliated CrCl_3 crystal. We tend to rule out the latter effect because the identical shape of the Cr multiplet in XAS experiments suggest very similar Cr coordination in the exfoliated and pristine crystal. Moreover, angle-dependent XMCD measurements show only minor differences between the normal and grazing incidence measurements that can be explained by shape anisotropy (i.e. demagnetizing field) in the high aspect ratio flakes (lateral size/thickness ratio of ~ 100).

The main effect observed after the exfoliation process on the CrCl_3 flakes, i.e. the increase of the saturation field, is thus caused by an enhancement of the antiferromagnetic coupling compared to the unexfoliated crystal. Following the classical treatment of Klein et al.^[21] and Wang et al.^[48], the strength of the interlayer interaction can be quantified by an effective exchange field H_e , which, together with the Zeeman and magnetic anisotropy interactions, contributes to the micromagnetic energy U per unit volume as in the following expression (in the cgs system):

$$U(H) = M_s \frac{H_e}{2} \sum_{i=1}^{N-1} \hat{m}_i \cdot \hat{m}_{i+1} - M_s \sum_{i=1}^N \vec{H} \cdot \hat{m}_i + K M_s^2 \sum_{i=1}^N \hat{m}_i \cdot \hat{z} \quad (\text{Equation 1})$$

where H is the in-plane applied field, M_s is the (volume) saturation magnetization, N the number of layers in the flake, \hat{m}_i is a unitary vector representing the magnetization orientation in the i -th layer, \hat{z} the unitary vector in the out-of-plane direction and K is the magnetocrystalline anisotropy constant, which is considered negligible in CrCl_3 .^[27,48] The field H_{FM} at which the antiferromagnetic-ferromagnetic transition occurs in the in-plane orientation is linked to the exchange field H_e and the number N of layers in the flake by the following expression:^[48]

$$H_{FM}(N) = 2H_e \cos^2 \left(\frac{\pi}{2N} \right) \quad (\text{Equation 2})$$

When the perpendicular orientation is considered, an additional $4\pi M_s$ term (in cgs units) is added to the right side of **Equation 2**, which accounts for the demagnetization field in the

flake. From Equation 2 it follows that the value of H_{FM} rapidly becomes insensitive to the number of layers, converging to the thick crystal value ($H_{FM}=2H_e$ for $N=\infty$). In fact, when $N=5$, as in a flake that is only 3.5nm thick, H_{FM} already reaches 90.5% of $2H_e$, while in the thickness range considered in this study (≈ 15 -30 nm for MFM, 10-50nm for XMCD), the model predicts H_{FM} to be $>99\%$ of the thick limit value. Therefore we can safely neglect the dependence on N in our case and attribute any change in H_{FM} to variations in H_e . The field H_{FM} can be determined using our XMCD data from the inflection point in the $M(H)$ or $I_{XMCD}(H)$ curves at 4 K, after correcting for the demagnetizing field $4\pi M_s$ in out-of-plane direction (see experimental section). We estimate $H_e \approx 1$ kOe ($H_{FM} \approx 2$ kOe) in bulk and ≈ 9 kOe ($H_{FM} \approx 18$ kOe) in exfoliated CrCl_3 crystal, resulting in a 9-fold increase in the value of H_e .

The agreement between the three techniques used in this work thus confirms that the increase of H_e is weakly dependent on the flake thickness as long as this is less than a few tens of nanometers. We can exclude that the observed increase is a surface effect, as the same field dependence was observed with a massive (SQUID) and a surface selective (XMCD) characterization technique. We remark that XAS analysis (Figure S8) confirmed negligible degradation of the exfoliated sample measured at the synchrotron. It is also unlikely that the observed properties derive from quantum confinement effects, since above a thickness of 10 layers, corresponding to > 5.8 nm in CrCl_3 , 2D crystals are expected to show bulk-like electronic properties.^[49,50]

Our observations are in agreement with the previous hypothesis that exfoliated CrCl_3 rearranges in a different lattice structure compared to the bulk material at low temperature, varying the inter-layer exchange interactions.^[10,21,25] This structural flexibility is probably due to the weak van der Waals interactions between the CrCl_3 layers, which determine a delicate energy balance governing the layer stacking. The nano-structuration of the CrCl_3 crystals may

cause a pinning of the high-temperature monoclinic structure at low temperature, as recently proposed,^[21] or possibly lead to novel metastable phases with the observed enhanced antiferromagnetic exchange. Nevertheless, we cannot exclude that other factors linked with the exfoliation process may affect the magnetic properties of the CrCl_3 flakes. Recent *ab initio* calculations have shown that a few % of Cr vacancies in CrCl_3 enhances the intra-layer ferromagnetic order and cause an insulator to half-metal electronic transition.^[51] It is also likely that the strain is different in the bulk and exfoliated material. *Ab initio* calculations on monolayers of the CrX_3 series found that a compressive strain of few % can switch the in-plane coupling from ferromagnetic to antiferromagnetic and increase the absolute value of the exchange interaction and the magneto-crystalline anisotropy by a factor of 2-3.^[52]

In conclusion, the magnetic properties of CrCl_3 flakes with a thickness of tens of nm ($\sim 10\text{-}50$ nm) and lateral sizes of several microns ($\sim 2\text{-}6$ μm) produced by micromechanical cleavage of bulk crystals were studied with multiple spectroscopic and magnetometric techniques. The exfoliated CrCl_3 sample has shown a reduction of the magnetic susceptibility and an increase of the ferromagnetic transition field H_{FM} at low temperature, compared to the bulk crystal. The effect was independently observed both on ensembles of CrCl_3 flakes by conventional superconducting quantum interference device (SQUID) magnetometry and synchrotron-based X-ray magnetic circular dichroism (XMCD) experiments, and on individual flakes by low-temperature magnetic force microscopy (MFM). These observations are in agreement with recent studies conducted with magneto-transport in tunnelling junctions^[21,28,29,48] and magneto-optical measurements,^[28] which highlighted that ultrathin flakes of chromium trihalides exhibit different magnetic interactions compared to the pristine bulk crystals.

Based on the experimental evidences, we can infer that the antiferromagnetic exchange interaction in the exfoliated phase is stronger than in the bulk crystal, suggesting several possible mechanisms for the explanation of this effect. It is worth noticing that low-

temperature MFM was applied here - for the first time - to spatially resolve field-dependent magnetization of van der Waals crystals with thickness of few tens of nanometres.

The joint experimental investigation by conventional magnetometry, XMCD and MFM provided compatible magnetization dependences, validating the use of MFM for the characterization of exfoliated van der Waals magnetic crystals. This study opens the way to the investigation of magnetic ordering and transitions in 2D crystals and heterostructures of even lower thickness with nanometric spatial resolution.

Supporting Information

Supporting Information is available from the Wiley Online Library or from the author.

Acknowledgements

The crystal growth at Princeton was supported by the ARO-sponsored MURI on Topological Insulators, grant number W911NF1210461. We acknowledge Fondazione Ente Cassa Risparmio di Firenze (progetto SPIN-E n. 2017.0730) and MIUR-Italy ("Progetto Dipartimenti di Eccellenza 2018-2022, ref B96C1700020008" allocated to Department of Chemistry "Ugo Schiff") for the economic support, SOLEIL for provision of synchrotron radiation facilities and all the DEIMOS staff for assistance in using the beamline. We thank the Clean Room Facility and the Materials Characterization Facility of the Italian Institute of Technology for support with sample preparation and material characterization.

Received: ((will be filled in by the editorial staff))

Revised: ((will be filled in by the editorial staff))

Published online: ((will be filled in by the editorial staff))

References

- [1] F. Bonaccorso, A. Lombardo, T. Hasan, Z. Sun, L. Colombo, A. C. Ferrari, *Mater. Today* **2012**, *15*, 564.
- [2] K. S. Novoselov, A. Mishchenko, A. Carvalho, A. H. Castro Neto, *Science* **2016**, *353*, 461.
- [3] A. C. Ferrari, F. Bonaccorso, V. Falko, K. S. Novoselov, S. Roche, P. Bøggild, S.

- Borini, F. Koppens, V. Palermo, N. Pugno, J. a. Garrido, R. Sordan, A. Bianco, L. Ballerini, M. Prato, E. Lidorikis, J. Kivioja, C. Marinelli, T. Ryhänen, A. Morpurgo, J. N. Coleman, V. Nicolosi, L. Colombo, A. Fert, M. Garcia-Hernandez, A. Bachtold, G. F. Schneider, F. Guinea, C. Dekker, M. Barbone, C. Galiotis, A. Grigorenko, G. Konstantatos, A. Kis, M. Katsnelson, C. W. J. Beenakker, L. Vandersypen, A. Loiseau, V. Morandi, D. Neumaier, E. Treossi, V. Pellegrini, M. Polini, A. Tredicucci, G. M. Williams, B. H. Hong, J. H. Ahn, J. M. Kim, H. Zirath, B. J. van Wees, H. van der Zant, L. Occhipinti, A. Di Matteo, I. a. Kinloch, T. Seyller, E. Quesnel, X. Feng, K. Teo, N. Rupesinghe, P. Hakonen, S. R. T. Neil, Q. Tannock, T. Löfwander, J. Kinaret, *Nanoscale* **2014**, 7, 4598.
- [4] B. Huang, G. Clark, E. Navarro-Moratalla, D. R. Klein, R. Cheng, K. L. Seyler, D. Zhong, E. Schmidgall, M. A. McGuire, D. H. Cobden, W. Yao, D. Xiao, P. Jarillo-Herrero, X. Xu, *Nature* **2017**, 546, 270.
- [5] Z. Fei, B. Huang, P. Malinowski, W. Wang, T. Song, J. Sanchez, W. Yao, D. Xiao, X. Zhu, A. F. May, W. Wu, D. H. Cobden, J. H. Chu, X. Xu, *Nat. Mater.* **2018**, 17, 778.
- [6] C. Gong, L. Li, Z. Li, H. Ji, A. Stern, Y. Xia, T. Cao, W. Bao, C. Wang, Y. Wang, Z. Q. Qiu, R. J. Cava, S. G. Louie, J. Xia, X. Zhang, *Nature* **2017**, 546, 265.
- [7] M. Bonilla, S. Kolekar, Y. Ma, H. C. Diaz, V. Kalappattil, R. Das, T. Eggers, H. R. Gutierrez, M.-H. Phan, M. Batzill, *Nat. Nanotechnol.* **2018**, 13, 289.
- [8] *Nat. Nanotechnol.* **2018**, 13, 269.
- [9] N. Samarth, *Nature* **2017**, 546, 216.
- [10] S. W. Jang, M. Y. Jeong, H. Yoon, S. Ryee, M. J. Han, *Phys. Rev. Mater.* **2019**, 3, 031001.
- [11] S. Jiang, L. Li, Z. Wang, K. F. Mak, J. Shan, *Nat. Nanotechnol.* **2018**, 13, 549.
- [12] K. L. Seyler, D. Zhong, D. R. Klein, S. Gao, X. Zhang, B. Huang, E. Navarro-Moratalla, L. Yang, D. H. Cobden, M. A. McGuire, W. Yao, D. Xiao, P. Jarillo-

- Herrero, X. Xu, *Nat. Phys.* **2018**, *14*, 277.
- [13] D. R. Klein, D. MacNeill, J. L. Lado, D. Soriano, E. Navarro-Moratalla, K. Watanabe, T. Taniguchi, S. Manni, P. Canfield, J. Fernández-Rossier, P. Jarillo-Herrero, *Science* **2018**, *360*, 1218.
- [14] Z. Wang, I. Gutiérrez-Lezama, N. Ubrig, M. Kroner, M. Gibertini, T. Taniguchi, K. Watanabe, A. Imamoğlu, E. Giannini, A. F. Morpurgo, *Nat. Commun.* **2018**, *9*, 2516.
- [15] T. Song, X. Cai, M. W.-Y. Tu, X. Zhang, B. Huang, N. P. Wilson, K. L. Seyler, L. Zhu, T. Taniguchi, K. Watanabe, M. A. McGuire, D. H. Cobden, D. Xiao, W. Yao, X. Xu, *Science* **2018**, *360*, 1214.
- [16] I. Zutic, J. Fabian, S. Das Sarma, *Rev. Mod. Phys.* **2004**, *76*, 323.
- [17] M. Grönke, B. Buschbeck, P. Schmidt, M. Valldor, S. Oswald, Q. Hao, A. Lubk, D. Wolf, U. Steiner, B. Büchner, S. Hampel, *Adv. Mater. Interfaces* **2019**, *6*, 1901410.
- [18] Y. Zhang, Y. Wang, P. Liao, K. Wang, Z. Huang, J. Liu, Q. Chen, J. Jiang, K. Wu, *ACS Nano* **2018**, *12*, 2991.
- [19] S. Jiang, J. Shan, K. F. Mak, *Nat. Mater.* **2018**, *17*, 406.
- [20] H. H. Kim, B. Yang, T. Patel, F. Sfigakis, C. Li, S. Tian, H. Lei, A. W. Tsen, *Nano Lett.* **2018**, *18*, 4885.
- [21] D. R. Klein, D. MacNeill, Q. Song, D. T. Larson, S. Fang, M. Xu, R. A. Ribeiro, P. C. Canfield, E. Kaxiras, R. Comin, P. Jarillo-Herrero, *Nat. Phys.* **2019**, *15*, 1255.
- [22] H. Wang, V. Eyert, U. Schwingenschlögl, *J. Phys. Condens. Matter* **2011**, *23*, 116003.
- [23] M. McGuire, *Crystals* **2017**, *7*, 121.
- [24] M. A. McGuire, H. Dixit, V. R. Cooper, B. C. Sales, *Chem. Mater.* **2015**, *27*, 612.
- [25] N. Sivadas, S. Okamoto, X. Xu, C. J. Fennie, D. Xiao, *Nano Lett.* **2018**, *18*, 7658.
- [26] D. Soriano, C. Cardoso, J. Fernández-Rossier, *Solid State Commun.* **2019**, *299*, 113662.
- [27] M. A. McGuire, G. Clark, S. KC, W. M. Chance, G. E. Jellison, V. R. Cooper, X. Xu, B. C. Sales, *Phys. Rev. Mater.* **2017**, *1*, 014001.

- [28] H. H. Kim, B. Yang, S. Li, S. Jiang, C. Jin, Z. Tao, G. Nichols, F. Sfigakis, S. Zhong, C. Li, S. Tian, D. G. Cory, G.-X. Miao, J. Shan, K. F. Mak, H. Lei, K. Sun, L. Zhao, A. W. Tsen, *Proc. Natl. Acad. Sci.* **2019**, *116*, 11131.
- [29] X. Cai, T. Song, N. P. Wilson, G. Clark, M. He, X. Zhang, T. Taniguchi, K. Watanabe, W. Yao, D. Xiao, M. A. McGuire, D. H. Cobden, X. Xu, *Nano Lett.* **2019**, *19*, 3993.
- [30] S. Blundell, *Magnetism in Condensed Matter*, Oxford University Press, Oxford, UK **2001**, pp. 85-110.
- [31] M. Bałanda, *Acta Phys. Pol. A* **2013**, *124*, 964.
- [32] A. Narath, H. L. Davis, *Phys. Rev.* **1965**, *137*, A163.
- [33] H. Bizette, A. Adam, C. Terrier, *C. R. Acad. Sci.* **1961**, *252*, 1571.
- [34] B. Kuhlowl, *Phys. status solidi* **1982**, *72*, 161.
- [35] M. C. Biesinger, C. Brown, J. R. Mycroft, R. D. Davidson, N. S. McIntyre, *Surf. Interface Anal.* **2004**, *36*, 1550.
- [36] G. Schütz, W. Wagner, W. Wilhelm, P. Kienle, R. Zeller, R. Frahm, G. Materlik, *Phys. Rev. Lett.* **1987**, *58*, 737.
- [37] J.-P. Kappler, E. Otero, W. Li, L. Joly, G. Schmerber, B. Muller, F. Scheurer, F. Leduc, B. Gobaut, L. Poggini, G. Serrano, F. Choueikani, E. Lhotel, A. Cornia, R. Sessoli, M. Mannini, M.-A. Arrio, P. Saintavit, P. Ohresser, *J. Synchrotron Radiat.* **2018**, *25*, 1727.
- [38] P. Ohresser, E. Otero, F. Choueikani, K. Chen, S. Stanescu, F. Deschamps, T. Moreno, F. Polack, B. Lagarde, J.-P. Daguerre, F. Marteau, F. Scheurer, L. Joly, J.-P. Kappler, B. Muller, O. Bunau, P. Saintavit, *Rev. Sci. Instrum.* **2014**, *85*, 013106.
- [39] É. Gaudry, P. Saintavit, F. Juillot, F. Bondioli, P. Ohresser, I. Letard, *Phys. Chem. Miner.* **2006**, *32*, 710.
- [40] M. Mannini, E. Tancini, L. Sorace, P. Saintavit, M.-A. Arrio, Y. Qian, E. Otero, D. Chiappe, L. Margheriti, J. C. Cezar, R. Sessoli, A. Cornia, *Inorg. Chem.* **2011**, *50*, 2911.

- [41] G. Vinai, A. Khare, D. S. Rana, E. Di Gennaro, B. Gobaut, R. Moroni, A. Y. Petrov, U. Scotti di Uccio, G. Rossi, F. Miletto Granozio, G. Panaccione, P. Torelli, *APL Mater.* **2015**, *3*, 116107.
- [42] V. Corradini, A. Ghirri, U. del Pennino, R. Biagi, V. A. Milway, G. Timco, F. Tuna, R. E. P. Winpenny, M. Affronte, *Dalt. Trans.* **2010**, *39*, 4928.
- [43] U. Hartmann, *Annu. Rev. Mater. Sci.* **1999**, *29*, 53.
- [44] M. Serri, M. Mannini, L. Poggini, E. Vélez-Fort, B. Cortigiani, P. Sainctavit, D. Rovai, A. Caneschi, R. Sessoli, *Nano Lett.* **2017**, *17*, 1899.
- [45] G. Lorusso, M. Jenkins, P. González-Monje, A. Arauzo, J. Sesé, D. Ruiz-Molina, O. Roubeau, M. Evangelisti, *Adv. Mater.* **2013**, *25*, 2984.
- [46] P. J. A. van Schendel, H. J. Hug, B. Stiefel, S. Martin, H.-J. Güntherodt, *J. Appl. Phys.* **2000**, *88*, 435.
- [47] S. Palleschi, G. D'Olimpio, P. Benassi, M. Nardone, R. Alfonsetti, G. Moccia, M. Renzelli, O. A. Cacioppo, A. Hichri, S. Jaziri, A. Politano, L. Ottaviano, *2D Mater.* **2019**, *7*, 025001.
- [48] Z. Wang, M. Gibertini, D. Dumcenco, T. Taniguchi, K. Watanabe, E. Giannini, A. F. Morpurgo, *Nat. Nanotechnol.* **2019**, *14*, 1116.
- [49] M. M. Otrokov, I. P. Rusinov, M. Blanco-Rey, M. Hoffmann, A. Y. Vyazovskaya, S. V. Eremeev, A. Ernst, P. M. Echenique, A. Arnau, E. V. Chulkov, *Phys. Rev. Lett.* **2019**, *122*, 107202.
- [50] A. C. Ferrari, J. C. Meyer, V. Scardaci, C. Casiraghi, M. Lazzeri, F. Mauri, S. Piscanec, D. Jiang, K. S. Novoselov, S. Roth, A. K. Geim, *Phys. Rev. Lett.* **2006**, *97*, 187401.
- [51] Y. Gao, J. Wang, Y. Li, M. Xia, Z. Li, F. Gao, *Phys. status solidi – Rapid Res. Lett.* **2018**, *12*, 1800105.
- [52] L. Webster, J.-A. Yan, *Phys. Rev. B* **2018**, *98*, 144411.

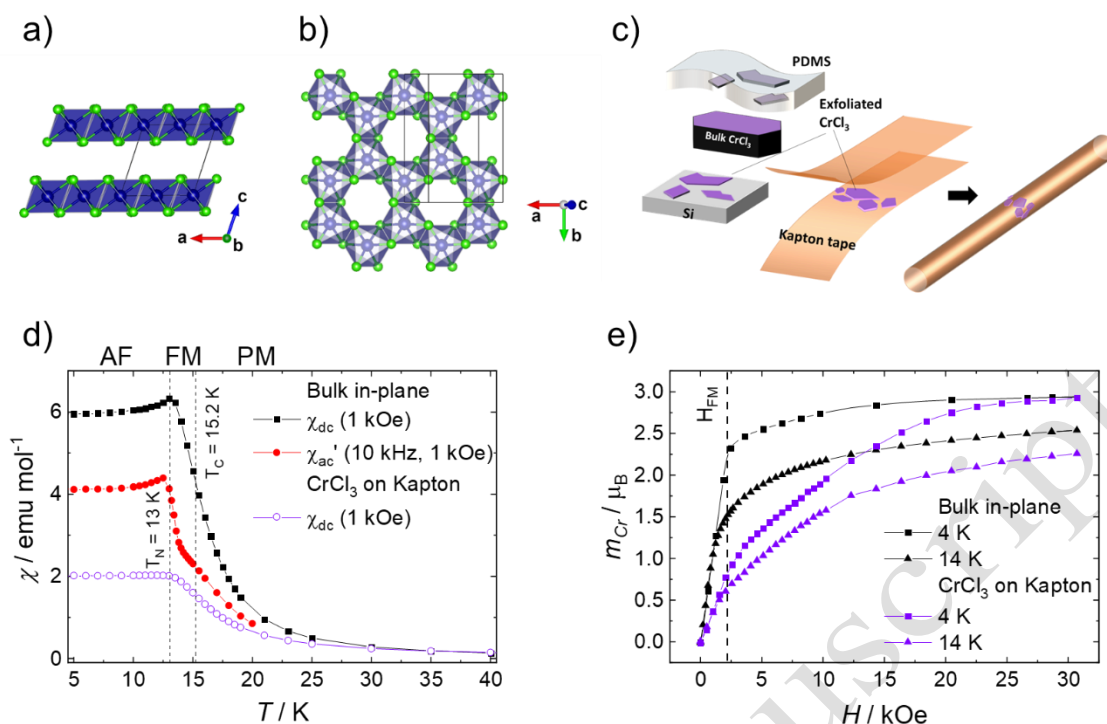


Figure 1. a) Lateral projection along the b axis of a CrCl_3 crystal in the monoclinic phase (green Cl, blue Cr. Octahedral coordination is highlighted). b) Top view of a single CrCl_3 layer; axes of the monoclinic cell are indicated. c) Schematic of the crystal exfoliation and flakes transfer process on Si and Kapton substrates; d) Temperature dependence of χ in bulk (black and red dots referred to dc and ac measurements, respectively) and exfoliated CrCl_3 (violet empty dots) measured with magnetic field in ab plane; e) isothermal magnetization curves of the bulk (black) and exfoliated (violet) CrCl_3 measured at 4 K (squares) and 14 K (triangles) with magnetic field in ab plane; the dashed line highlights the field H_{FM} corresponding to the transition to a ferromagnetic-like state in bulk at 4K.

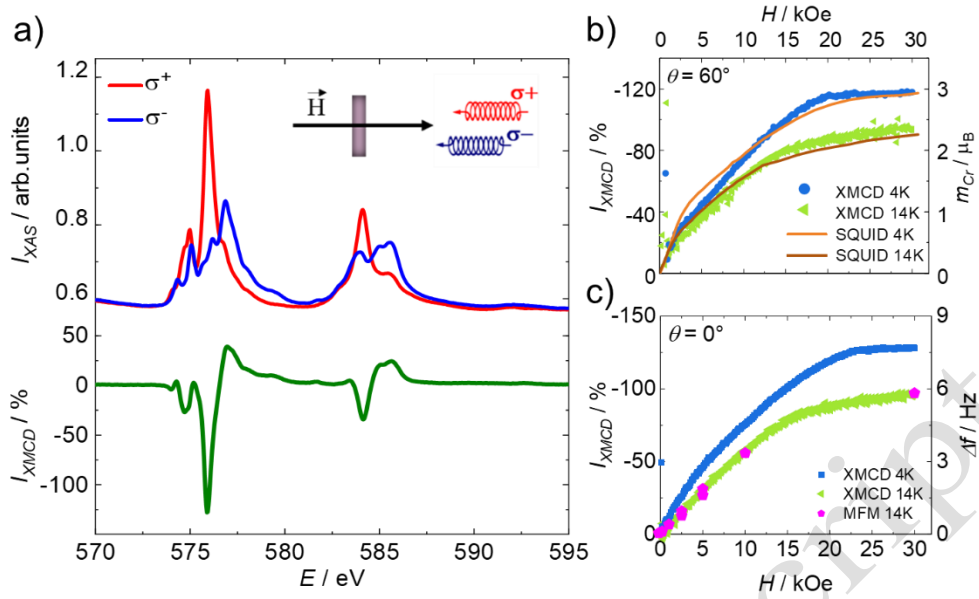


Figure 2. a) XAS and XMCD spectra obtained on the exfoliated sample on Si at the $\text{CrL}_{2,3}$ edge with $H = 30$ kOe, $T = 4$ K and normal incidence ($\theta = 0^\circ$), red line and blue line are σ^+ and σ^- respectively, green line is XMCD; b) isothermal (4 K blue, 14 K green) XMCD measurements at grazing incidence ($\theta = 60^\circ$) of the CrCl_3 flakes on Si, compared with SQUID magnetometry (4K orange, 14K brown) of the flakes on Kapton; c) isothermal (4 K blue, 14 K green) XMCD measurements at normal incidence of the CrCl_3 flakes on Si, compared with field dependence of the MFM contrast (magenta points).

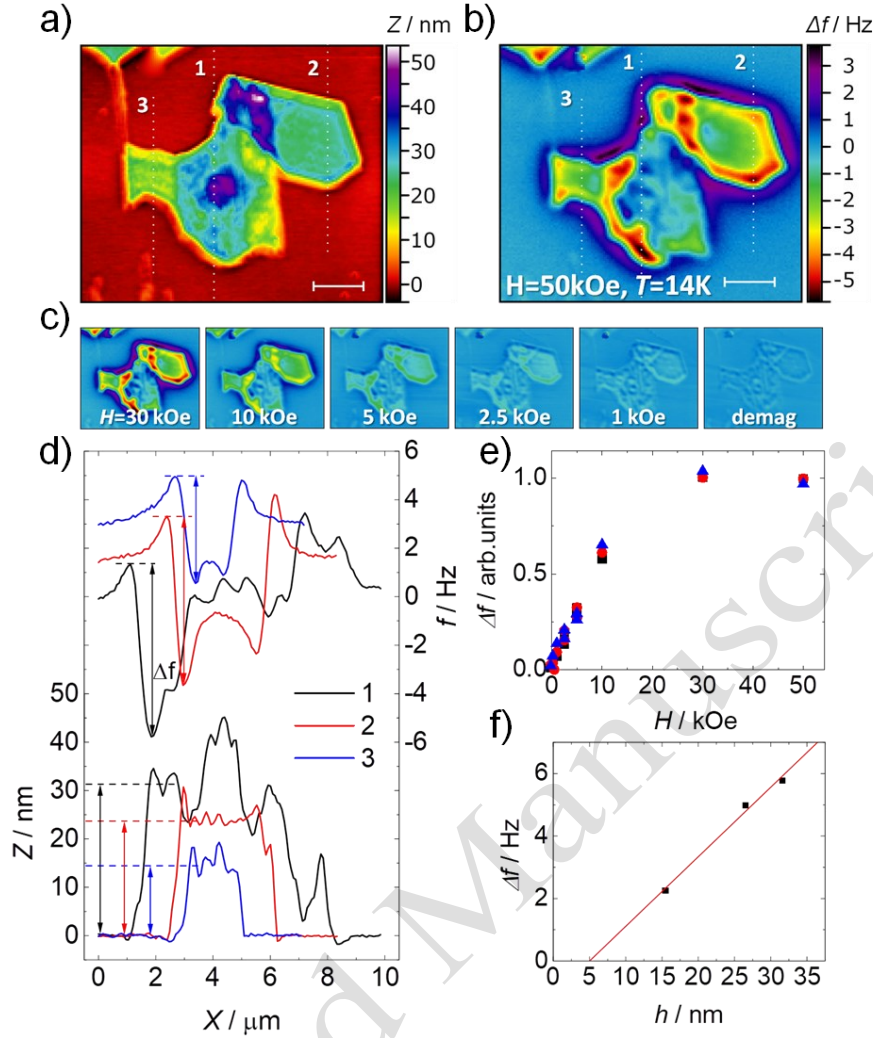


Figure 3. a) AFM image of exfoliated CrCl_3 flakes on Si; b) MFM image of the region in a), measured at 50 kOe and 14 K; the numbered dotted lines in a) and b) indicate the profiles along which the MFM signal was analysed; c) MFM images acquired at 14K and magnetic fields between 30kOe and 0Oe (demagnetized state); d) MFM contrast (top) and AFM topography (bottom) along the profiles indicated in a) and b); e) normalized MFM contrast in the three profiles as a function of applied field at 14 K; f) correlation between the thickness of the flakes along the three profiles and the respective saturation MFM signal measured at 50 kOe and 14K.